

Chaotic Attractors with A Single Non-Hyperbolic Fixed Point in A Class of Two-Dimensional Maps

Liping Zhang *, Haibo Jiang

School of Mathematics and Statistics, Yancheng Teachers University, Yancheng 224002, China

(Received 2 November 2017, accepted 10 January 2018)

Abstract: This paper explores some elementary quadratic chaotic maps with a single non-hyperbolic fixed point by performing a systematic computer search. The existence of the non-hyperbolic fixed point in these maps is investigated, and several examples are illustrated by using various numerical methods, such as the phase-basin portraits, the Lyapunov exponents, and the maximum of the local Lyapunov dimensions. For these two-dimensional maps, there is no repelling fixed point, so the Marotto's theorem is invalid. Bifurcation analysis is carried out to show the occurrence of chaotic attractors with a single non-hyperbolic fixed point.

Keywords: two-dimensional maps; fixed point; stability; bifurcation analysis; coexistence

1 Introduction

According to the Leonov-Kuznetsov classification for attractors [1–5] from a computational point of view, the attractors are divided into two categories, i.e. hidden attractors and self-excited attractors. The attractors are hidden if their basins of attraction do not intersect with small neighborhoods of equilibria; Otherwise, the attractors are self-excited attractors[1–5]. The well-known chaotic attractors generated from Lorenz system [6], Rössler system [7], chaotic flows [8], and Chua's circuit [9] are self-excited attractors. Self-excited attractors can be localized by employing usual numerical methods. However, there is no good way to localize the hidden attractors. So hidden attractors have received considerable attention from the research community, and they have been found in many dynamical systems, such as the Chua system [1–3], the drilling system [4], and the automatic control systems with piecewise-linear non-linearity [5]. Very recently, hidden chaotic attractors have been explored in continuous dynamical systems with different structure of equilibria [10–25]. However, there are very few results on hidden attractors in discrete-time maps. In [26], hidden stable periodic solutions were shown for three second-order counterexamples to the discrete-time Kalman conjecture. In [27], hidden attractors in an one-dimensional map were studied by extending the Logistic map. In [28, 29], a schematic method was proposed to explore the hidden chaotic attractors in a class of two-dimensional and three-dimensional maps. Until now, the research work on hidden attractors in discrete-time maps is still raw, and there are many unexplored openings [30, 31].

For continuous dynamical systems, the proof of existence of chaos has been studied extensively in the literature [32, 33]. The commonly used analytic criteria for proving chaos in autonomous systems are the Smale horseshoe and the Shilnikov condition [32, 33]. According to the Shilnikov condition, chaos can be classified into four types: homoclinic chaos, heteroclinic chaos, a combination of homoclinic and heteroclinic chaos, and chaos without homoclinic or heteroclinic orbits [34]. However, in some special cases of strange attractors, the Shilnikov condition does not hold. For example, Wei et al. [34] studied a class of jerk equations with quadratic nonlinearities which can generate a catalog of nine elementary dissipative chaotic flows with the unusual feature of having a single non-hyperbolic equilibrium. For such unusual systems, the Shilnikov method cannot be used to verify chaos as they could have neither homoclinic nor heteroclinic orbits.

On the other hand, the proof of existence of chaos in discrete-time maps has also received great attention from researchers, e.g. [35–43]. In [35], Li and Yorke introduced the first mathematical definition of chaos and established a

*Corresponding author. E-mail address: yctczlp@126.com

very simple criterion for one-dimensional discrete dynamical systems, namely, “period three implies chaos” for brevity. Later on, Marotto [36] extended the Li-Yorke’s theorem of chaos from one-dimension to multi-dimension by introducing the notion of snapback repeller, and Li and Chen [37, 38] proposed an improved version of the Marotto’s theorem. In [39], Marotto redefined the snapback repeller for validating his theorem due to a technical flaw in the original derivation. Marotto’s theorem is essential in analytic theory of chaos and effective for identifying the chaotic regime of dynamical systems. In [40–42], several numerical methods for finding the snapback repellers were proposed based on the Marotto’s theorem. However, there must exist a fixed point called a repelling fixed point which at least satisfies that all eigenvalues of the Jacobian matrix must exceed one in magnitude (quoted from the definition in [39]). Some other numerical methods for proofing onset of chaos (e.g. the computed-assist proof of chaos [43–45]) in maps were developed. In [44], Li and Yang proposed an efficient method for finding horseshoes in dynamical systems by using several simple results on topological horseshoes, but the use of the method may depend on user’s trials and experiences.

This paper will explore some elementary quadratic chaotic maps with a single non-hyperbolic fixed point via performing an exhaustive computer search [46, 47]. Typical attractors will be presented in the phase-basin portrait and numerically analyzed by the Lyapunov exponents and the Kaplan-Yorke dimension. Our exploration will show that there is no repelling fixed point in these maps, so the Marotto’s theorem is invalid. Bifurcation analysis will be carried out for considering the occurrence of chaotic attractor with a single non-hyperbolic fixed point. The findings in this paper will be useful for researchers to understand the dynamical mechanism of discrete-time maps. The rest of this paper is organized as follows. In Section 2, the mathematical model of a class of two-dimensional maps is introduced, and the existence of non-hyperbolic fixed points is studied. The chaotic attractors with a single non-hyperbolic fixed point are investigated in Section 3. Finally, some conclusions are drawn in Section 4.

2 System model and non-hyperbolic fixed points

Following the work in [28], we consider a class of two-dimensional maps which can be described by the following difference equation

$$\begin{cases} x_{k+1} = y_k \\ y_{k+1} = a_1x_k + a_2y_k + a_3x_k^2 + a_4y_k^2 + a_5x_ky_k + a_6 \end{cases} \quad (1)$$

where $a_1, a_2, a_3, a_4, a_5, a_6$ are real coefficients to be determined later, x and y are system states.

The fixed point (x^*, y^*) must satisfy the following conditions

$$\begin{cases} x = y \\ y = a_1x + a_2y + a_3x^2 + a_4y^2 + a_5xy + a_6 \end{cases} \quad (2)$$

Then the problem of finding fixed points can be transformed into the following equation with respect to y

$$(a_3 + a_4 + a_5)y^2 + (a_1 + a_2 - 1)y + a_6 = 0 \quad (3)$$

The Jacobian matrix of the map evaluated at the fixed point (x^*, y^*) is

$$J = \begin{bmatrix} 0 & 1 \\ a_1 + 2a_3x^* + a_5y^* & a_2 + 2a_4y^* + a_5x^* \end{bmatrix} \quad (4)$$

The characteristic equation is

$$\det(\lambda I - J) = \lambda^2 - \text{tr}(J)\lambda + \det(J) = 0 \quad (5)$$

where $\det(J) = -(a_1 + 2a_3x^* + a_5y^*)$ is the determinant of the Jacobian matrix and $\text{tr}(J) = a_2 + 2a_4y^* + a_5x^*$ is the trace of the Jacobian matrix. According to the theory of matrix, the sum of eigenvalues of the Jacobian matrix is equal to $\text{tr}(J)$ and the product of eigenvalues of the Jacobian matrix is equal to $\det(J)$. The eigenvalues λ_1, λ_2 of J are called multipliers of the fixed point. Let n_-, n_0 and n_+ be the numbers of multipliers of the fixed point (x^*, y^*) lying inside, on, and outside the unit circle $\{\lambda \in \mathbb{C} : |\lambda| = 1\}$, respectively.

Definition 1 (Definition 2.10 in [48]) A fixed point (x^*, y^*) is called hyperbolic if $n_0 = 0$, that is, if there is no eigenvalue of the Jacobian matrix evaluated at this fixed point on the unit circle. Otherwise, the fixed point is called non-hyperbolic, that is, there is at least one eigenvalue of the Jacobian matrix evaluated at the fixed point on the unit circle.

Assume that there exists a fixed point (x^*, y^*) of map (1). This fixed point is stable if the roots λ_1, λ_2 of the characteristic equation satisfy that $|\lambda_{1,2}| < 1$. If $a_3 + a_4 + a_5 \neq 0$, $\Delta = (a_1 + a_2 - 1)^2 - 4(a_3 + a_4 + a_5)a_6$ is denoted as the discriminant of Eq. (3). In the following, the existence of the non-hyperbolic fixed point will be determined.

2.1 Single non-hyperbolic fixed point I (SNF I)

As shown in [28], if $a_3 + a_4 + a_5 \neq 0$ and $\Delta = 0$, Eq.(3) has a pair of equal roots $y_1 = y_2 = -\frac{a_1+a_2-1}{2(a_3+a_4+a_5)}$. So the map (1) has a single fixed point (x^*, y^*) , where $x^* = y^* = -\frac{a_1+a_2-1}{2(a_3+a_4+a_5)}$. Since $\text{tr}(J) = \det(J) + 1$, there is a real root $\lambda = 1$. Thus, according to **Definition 1**, this fixed point is non-hyperbolic.

2.2 Single non-hyperbolic fixed point II (SNF II)

As shown in [28], if $a_3 + a_4 + a_5 = 0$ and $a_1 + a_2 - 1 \neq 0$, Eq. (3) has a single solution $y = -\frac{a_6}{a_1+a_2-1}$, and the map (1) has a single fixed point (x^*, y^*) , where $x^* = y^* = -\frac{a_6}{a_1+a_2-1}$. This fixed point is non-hyperbolic if at least one of the eigenvalues λ_1, λ_2 of the Jacobian matrix J lies on the unit circle. From the stability theory of two-dimensional discrete systems [49–51], the fixed point (x^*, y^*) is non-hyperbolic if one of the following conditions is satisfied

$$\begin{cases} C_1 : \det(J) - 1 = 0, |\text{tr}(J)| < 2, \\ C_2 : \text{tr}(J) - \det(J) - 1 = 0, \\ C_3 : \text{tr}(J) + \det(J) + 1 = 0, \end{cases}$$

which leads to

$$\begin{cases} C'_1 : (a_1 - a_1a_2 + 2a_3a_6 + a_5a_6 - a_1^2)/(a_1 + a_2 - 1) - 1 = 0, \\ \quad |a_2 - (2a_4a_6)/(a_1 + a_2 - 1) - (a_5a_6)/(a_1 + a_2 - 1)| < 2, \\ C'_2 : a_2 - (a_1 - a_1a_2 + 2a_3a_6 + a_5a_6 - a_1^2)/(a_1 + a_2 - 1) \\ \quad - (2a_4a_6)/(a_1 + a_2 - 1) - (a_5a_6)/(a_1 + a_2 - 1) - 1 = 0, \\ C'_3 : a_2 + (a_1 - a_1a_2 + 2a_3a_6 + a_5a_6 - a_1^2)/(a_1 + a_2 - 1) \\ \quad - (2a_4a_6)/(a_1 + a_2 - 1) - (a_5a_6)/(a_1 + a_2 - 1) + 1 = 0. \end{cases}$$

As shown in [49–51], if the condition C_1 is satisfied, the Jacobian matrix J calculated at this fixed point has two complex eigenvalues with $|\lambda_1| = |\lambda_2| = 1$; if the condition C_2 is satisfied, the Jacobian matrix J evaluated at this fixed point has a real eigenvalue 1, i.e., $\lambda_1 = 1$; if the condition C_3 is satisfied, the Jacobian matrix J calculated at this fixed point has a real eigenvalue -1, i.e., $\lambda_1 = -1$. Thus, according to **Definition 1**, this fixed point is non-hyperbolic. However, by using the command “simplify” in the scientific computing software MATLAB, there is a contraction in $a_3+a_4+a_5 = 0$, $a_1 + a_2 - 1 \neq 0$ and the condition C_2 . Therefore, this reveals that the map cannot have this type of fixed point for which the Jacobian matrix J has a real eigenvalue of 1.

3 Chaotic attractors with a single non-hyperbolic fixed point

In this section, a systematic computer search program [13, 18, 46] was used to explore the chaotic attractors with a single non-hyperbolic fixed point.

3.1 Chaotic attractors with a single non-hyperbolic fixed point I (SNF I)

Table 1: Examples of the two-dimensional maps with SNF I

Cases	Maps	FP	λ_i	(x_0, y_0)	Les	$\overline{\dim}_L$
SNFI ₁	$\begin{cases} x_{k+1} = y_k \\ y_{k+1} = -y_k + y_k^2 - 3.5x_k y_k - 0.4 \end{cases}$	-0.4 -0.4	1 -1.4	-0.23 -0.16	0.1754 -0.4597	1.3821
SNFI ₂	$\begin{cases} x_{k+1} = y_k \\ y_{k+1} = 1.78x_k - 0.07x_k^2 - 0.32x_k y_k - 0.39 \end{cases}$	1 1	1 -1.32	4.11 2.03	0.1631 -0.6311	1.2586
SNFI ₃	$\begin{cases} x_{k+1} = y_k \\ y_{k+1} = -0.89x_k^2 - 1.6y_k^2 + 2.74x_k y_k + 1 \end{cases}$	2 2	1 -1.92	0.36 0.87	0.1939 -0.3050	1.6355
SNFI ₄	$\begin{cases} x_{k+1} = y_k \\ y_{k+1} = 1.46x_k - 0.46y_k + 0.26x_k^2 + 0.87x_k y_k \end{cases}$	0 0	1 -1.46	-0.04 0.28	0.3001 -0.4320	1.6953

Four typical examples of the two-dimensional maps are presented in Table 1 at where the fixed points (FP), the eigenvalues of the Jacobian matrix at the fixed points (λ_i), the initial values (x_0, y_0) , the Lyapunov exponents (Les), and the maximum of the local Lyapunov dimensions $\overline{\dim}_L$ are given. The Lyapunov exponents and the maximum of the

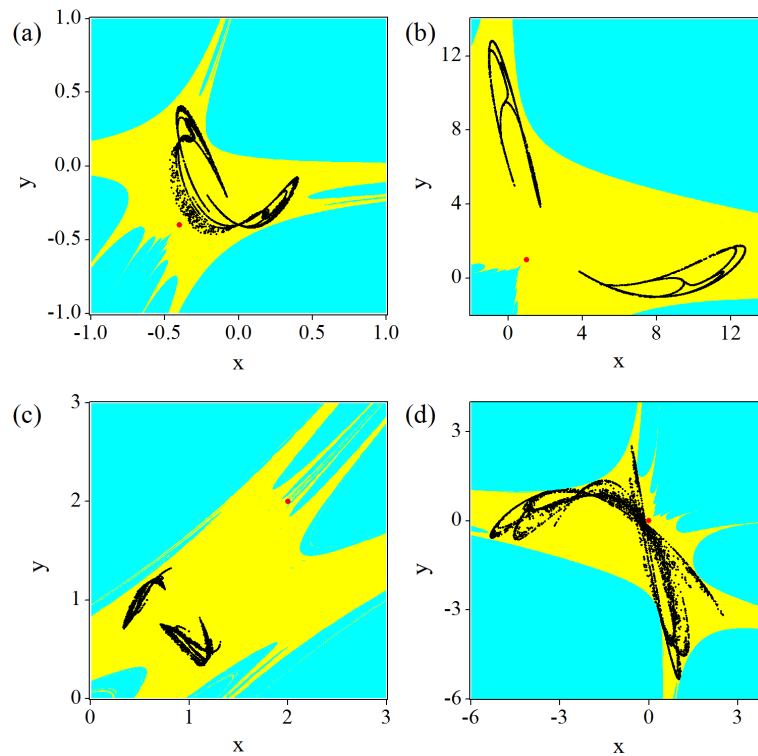


Figure 1: (colour online) Phase-basin portraits of the maps listed in Table 1: (a) SNFI₁, (b) SNFI₂, (c) SNFI₃, and (d) SNFI₄. Chaotic attractors and non-hyperbolic fixed points are denoted by black and red dots, respectively. The basins of unbound and chaotic attractors are shown in cyan and yellow, respectively.

local Lyapunov dimensions of the chaotic attractors were computed by using the same method given in [52–57]. If the Lyapunov exponents of the point $p_0 = (x_0, y_0)$ on the chaotic attractors are $L_1(p_0)$ and $L_2(p_0)$, i.e., $L_1(p_0) > 0$ and $L_2(p_0) < 0$, the local Lyapunov (Kaplan-Yorke) dimension $\dim_L p_0$ can be given as $\dim_L p_0 = 1 - L_1(p_0)/L_2(p_0)$. In this paper, a grid of points on chaotic attractors were used to find the maximum of the local Lyapunov dimensions, i.e., $\bar{\dim}_L = \max_{p_0 \in B} (\dim_L p_0)$, where B was the set of points on chaotic attractors with a grid step $h = 0.1$ of the phase space. In the reorthogonalization procedure, the time-step and the number of iterations were chosen as 10 and 10^7 , respectively. Since all the maps in Table 1 satisfy $a_3 + a_4 + a_5 \neq 0$ and $\Delta = 0$, they all have a single fixed point. Moreover, one of their eigenvalues of the Jacobian matrix at the fixed points is 1, so these fixed points are all non-hyperbolic. It can be seen from Table 1 that all the maximal Lyapunov exponents are positive, so all the attractors in Fig. 1 obtained by the given initial values are chaotic.

The phase-basin portraits for the maps listed in Table 1 are presented in Fig. 1, where the chaotic attractors and the fixed points are shown by black and red dots, and the basins of unbound and the chaotic attractors are depicted in cyan and white, respectively. From Fig.1, it can be seen that all the maps listed in Table 1 do not have other attractor except the chaotic ones.

In order to investigate the occurrence of chaotic attractor with the single non-hyperbolic fixed point, bifurcation analysis for the map SNFI₁ with respect to the branching parameter a_6 was carried out. The bifurcation and the Lyapunov exponents diagrams are shown in Fig. 2, where the stable solutions are denoted by black dots, and the unstable fixed points, period-2 and period-4 solutions are marked by magenta, blue, and green dashed lines, respectively. It can be seen from Fig. 2(a) that stable (black dots) and unstable (magenta dashed line) fixed points coexist for $a_6 \in (0, 0.05]$. At $a_6 = 0$, there is a period-doubling bifurcation, so the stable fixed point loses stability and a stable period-2 solution emerges. As a_6 decreases, the map undergoes a period-doubling bifurcation at $a_6 = -0.2123$ and the period-2 solution bifurcates into a stable period-4 solution. When $a_6 = -0.3531$, the stable period-4 solution loses stability again via a period-doubling bifurcation followed by a period-8 solution. Thereafter the map experiences a period-doubling bifurcation cascade leading

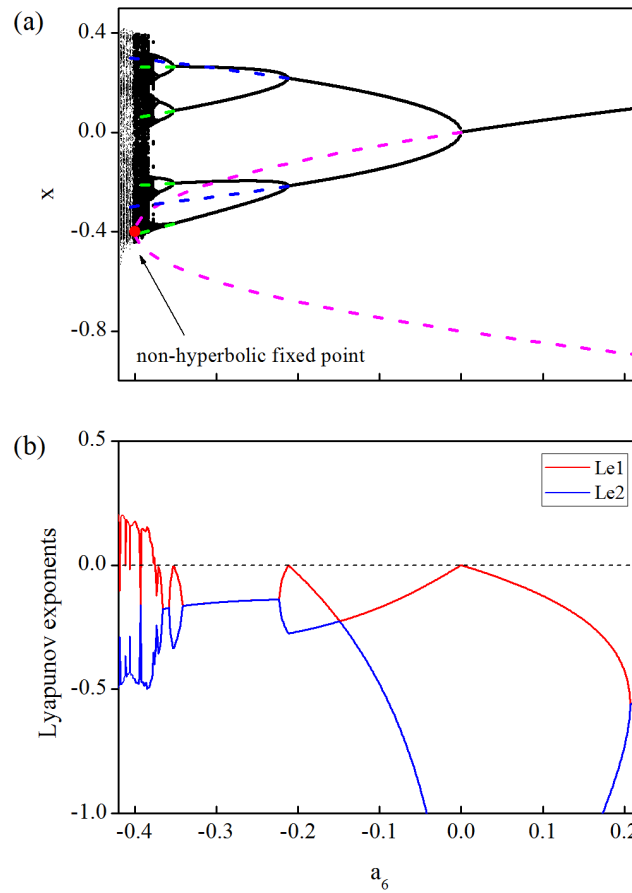


Figure 2: (colour online) (a) Bifurcation and (b) Lyapunov exponents diagrams of the map SNFI_1 . Stable solutions are denoted by black dots, and unstable fixed points, period-2 and period-4 solutions are marked by magenta, blue, and green dashed lines, respectively. The non-hyperbolic fixed point is shown by a red dot. The largest Lyapunov exponent (Le1) and the smallest Lyapunov exponent (Le2) are shown in red and blue lines, respectively.

to chaos. For the up branch of the unstable fixed points, our calculations show that the absolute values of their eigenvalues satisfy $|\lambda_1| > 1$ and $|\lambda_2| < 1$ when $a_6 \in (-0.4, 0]$. At $a_6 = -0.4$, one of the eigenvalues becomes one, i.e., $\lambda_1 > 1$ and $\lambda_2 = 1$, so this unstable fixed point is a non-hyperbolic fixed point. For the down branch of the unstable fixed points, all the absolute values of their eigenvalues are greater than one, i.e., $|\lambda_{1,2}| > 1$ when $a_6 \in (-0.4, 0.05]$. Therefore, the occurrence of the chaotic attractors with a single non-hyperbolic fixed point is validated by this bifurcation analysis.

3.2 Chaotic attractors with a single non-hyperbolic fixed point II (SNF II)

Four typical examples of the two-dimensional maps are presented in Table 2, where the fixed points (FP), the eigenvalues of the Jacobian matrix calculated at the fixed points (λ_i), the initial values (x_0, y_0), the Lyapunov exponents (Les), and the maximum of the local Lyapunov dimensions $\overline{\dim}_L$ are given. The phase-basin portraits of these two-dimensional maps are shown in Fig. 3. Since all these maps satisfy $a_3 + a_4 + a_5 = 0$ and $a_1 + a_2 - 1 \neq 0$, they all have a single fixed point. The coefficients of the maps SNFII_1 and SNFII_2 satisfy the condition C_1 . The eigenvalues of the Jacobian matrix at the fixed points of the maps SNFII_1 and SNFII_2 are complex and their modules are 1. Thus, these fixed points are all non-hyperbolic. The coefficients of the maps SNFII_3 and SNFII_4 satisfy the condition C_3 . One of the eigenvalues of the Jacobian matrix calculated at the fixed points of the maps SNFII_3 and SNFII_4 is -1. Thus, these fixed points are all non-hyperbolic. It can be seen from Table 2 that all the maximal Lyapunov exponents are positive, so all the attractors shown in Fig. 3 obtained by the given initial values are chaotic.

Table 2: Examples of the two-dimensional maps with SNF II

Cases	Maps	FP	λ_i	$ \lambda_i $	(x_0, y_0)	Les	$\dim_{\mathcal{L}}$
SNFII ₁	$\begin{cases} x_{k+1} = y_k \\ y_{k+1} = -x_k + 0.31y_k \\ -0.04x_k^2 - 0.63y_k^2 + 0.67x_k y_k \end{cases}$	$\begin{matrix} 0 \\ 0 \end{matrix}$	$\begin{matrix} 0.1550 + 0.9879i \\ 0.1550 - 0.9879i \end{matrix}$	$\begin{matrix} 1 \\ 1 \end{matrix}$	$\begin{matrix} -0.47 \\ -2.01 \end{matrix}$	$\begin{matrix} 0.1309 \\ -0.7453 \end{matrix}$	1.1756
SNFII ₂	$\begin{cases} x_{k+1} = y_k \\ y_{k+1} = -x_k - 0.55y_k \\ -0.46x_k^2 + 0.76y_k^2 - 0.3x_k y_k \end{cases}$	$\begin{matrix} 0 \\ 0 \end{matrix}$	$\begin{matrix} -0.2750 + 0.9614i \\ -0.2750 - 0.9614i \end{matrix}$	$\begin{matrix} 1 \\ 1 \end{matrix}$	$\begin{matrix} -1.61 \\ 0.89 \end{matrix}$	$\begin{matrix} 0.1228 \\ -0.5214 \end{matrix}$	1.2357
SNFII ₃	$\begin{cases} x_{k+1} = y_k \\ y_{k+1} = 0.38x_k - 0.62y_k \\ -0.55x_k^2 + y_k^2 - 0.45x_k y_k \end{cases}$	$\begin{matrix} 0 \\ 0 \end{matrix}$	$\begin{matrix} -1 \\ 0.38 \end{matrix}$	$\begin{matrix} 1 \\ 0.38 \end{matrix}$	$\begin{matrix} 0.93 \\ -0.85 \end{matrix}$	$\begin{matrix} 0.1114 \\ -0.5386 \end{matrix}$	1.2069
SNFII ₄	$\begin{cases} x_{k+1} = y_k \\ y_{k+1} = -1.19x_k - 2.19y_k \\ -0.3x_k^2 + 0.33y_k^2 - 0.03x_k y_k \end{cases}$	$\begin{matrix} 0 \\ 0 \end{matrix}$	$\begin{matrix} -1 \\ -1.19 \end{matrix}$	$\begin{matrix} 1 \\ 1.19 \end{matrix}$	$\begin{matrix} -1.19 \\ 0.81 \end{matrix}$	$\begin{matrix} 0.0622 \\ -0.4038 \end{matrix}$	1.1542

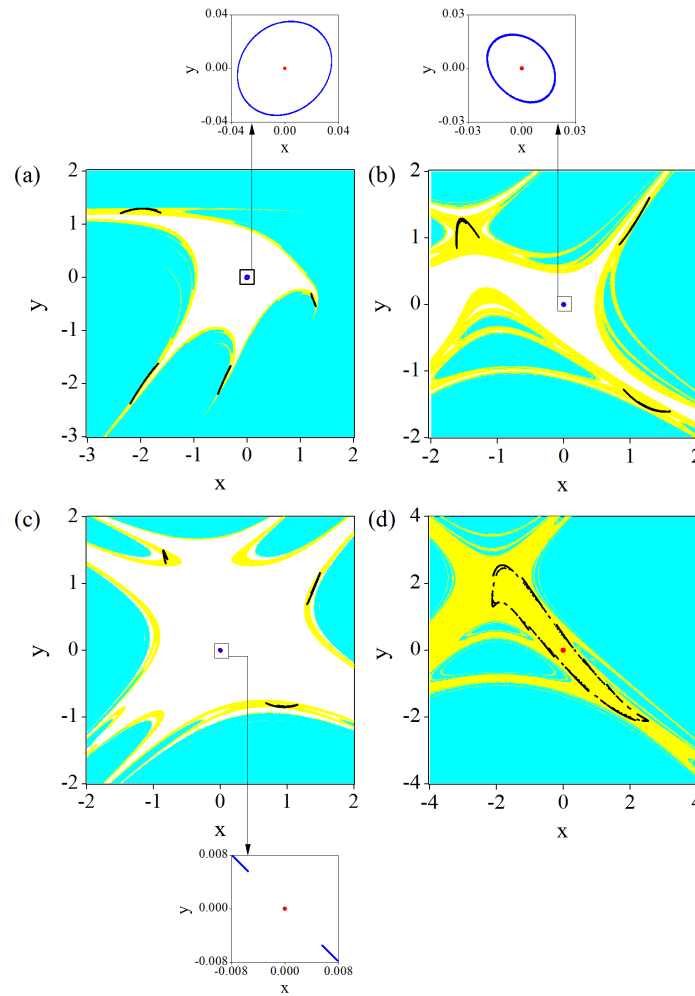


Figure 3: (colour online) Phase-basin portraits of the maps listed in Table 2: (a) SNFII₁, (b) SNFII₂, (c) SNFII₃, and (d) SNFII₄. Chaotic attractors, quasi-periodic attractors and non-hyperbolic fixed points are denoted by black, blue and red dots, respectively. The basins of unbound, quasi-periodic attractors and chaotic attractors are shown in cyan, white and yellow, respectively. The blow-up windows show the coexisting quasi-periodic attractors near the non-hyperbolic fixed point (0, 0).

In Fig. 3, the chaotic attractors, the quasi-periodic attractors, and the non-hyperbolic fixed points are denoted by black, blue, and red dots, and the basins of unbound, the quasi-periodic attractors, and the chaotic attractors are shown in cyan, white, and yellow, respectively. The blow-up windows show the coexisting attractors near the non-hyperbolic fixed point

$(0, 0)$. As can be seen from Fig. 3(a)-(c), the basins of chaotic attractors of the maps SNFII₁, SNFII₂ and SNFII₃ are smaller than the basins of the coexisting quasi-periodic attractors shown in the blow-up windows. The quasi-periodic attractors of the maps SNFII₁ and SNFII₂ are small and form circles around the non-hyperbolic fixed point $(0, 0)$. At this parameter, the map undergoes a Neimark-Sacker bifurcation and these quasi-periodic attractors occur. For the map SNFII₃, the largest Lyapunov exponent of the attractor near the non-hyperbolic fixed point $(0, 0)$ is closely near zero, so the attractor is quasi-periodic. However, the quasi-periodic attractors of the map SNFII₃ are too small to show two circles. From Fig. 3(d), no coexisting attractor has been observed.

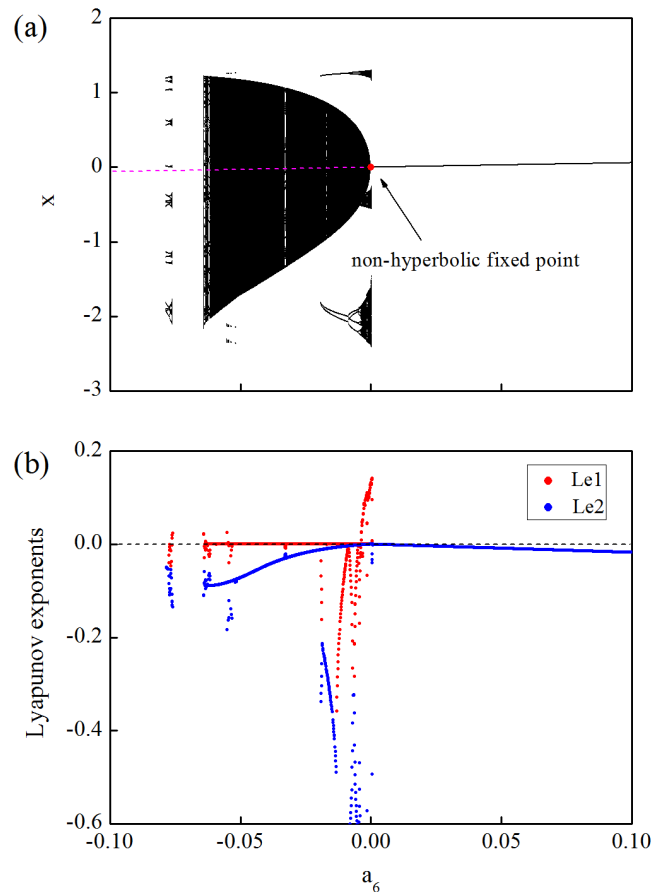


Figure 4: (colour online) (a) Bifurcation and (b) Lyapunov exponents diagrams of the map SNFII₁. Stable solutions are denoted by black dots, unstable fixed points are marked by magenta dashed lines, and the non-hyperbolic fixed point is shown by a red dot. The largest Lyapunov exponent (Le1) and the smallest Lyapunov exponent (Le2) are shown in red and blue dots, respectively.

In order to investigate the occurrence of the chaotic attractors with a single non-hyperbolic fixed point, bifurcation analyses with respect to the parameter a_6 for the maps SNFII₁ and SNFII₃ were carried out. The bifurcation and the Lyapunov exponents diagrams for the map SNFII₁ are shown in Fig. 4, where the stable solutions are denoted by black dots, the unstable fixed points are marked by magenta dashed lines, and the non-hyperbolic fixed point is shown by a red dot. As the parameter a_6 decreases from 0.1, the map undergoes a Neimark-Sacker bifurcation at $a_6 = 0$ and the stable fixed point bifurcates into a quasi-periodic attractor. So, at $a_6 = 0$, the fixed point is non-hyperbolic. Furthermore, there is a coexisting chaotic attractor which is led by a period-doubling bifurcation cascade from other branch of periodic solutions. As the parameter a_6 decreases, the fixed point becomes unstable. The Lyapunov exponents of the map SNFII₁ shown in Fig. 4(b) verify this numerical results.

The bifurcation and the Lyapunov exponents diagrams for the map SNFII₃ are shown in Fig. 5, where stable solutions are denoted by black dots, unstable fixed points are marked by magenta dashed lines, and non-hyperbolic fixed point

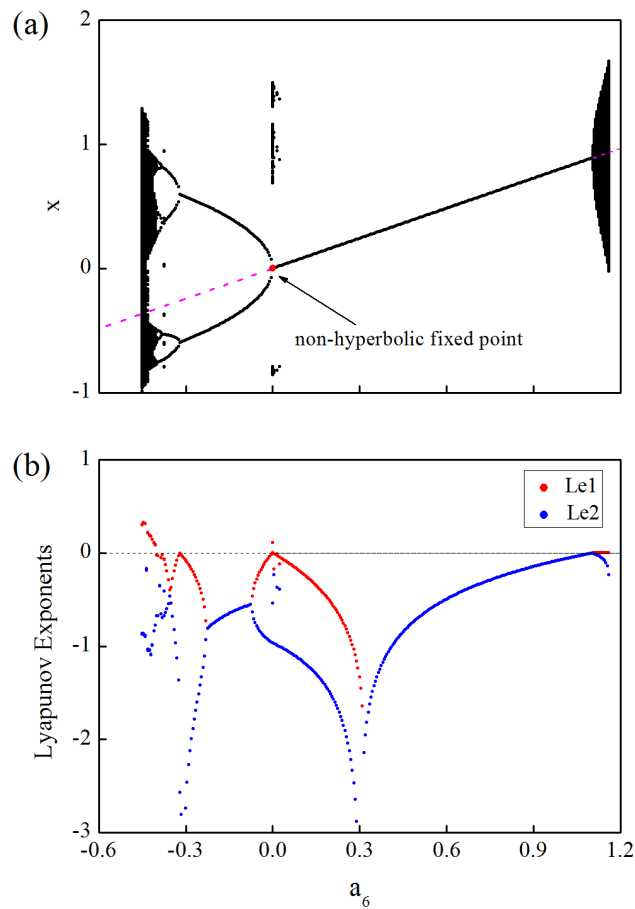


Figure 5: (colour online) (a) Bifurcation and (b) Lyapunov exponents diagrams of the map SNFII_3 . Stable solutions are denoted by black dots, unstable fixed points are marked by magenta lines, and the non-hyperbolic fixed point is shown by a red dot. The largest Lyapunov exponent (Le1) and the smallest Lyapunov exponent (Le2) are shown in red and blue dots, respectively.

is shown by a red dot. As can be seen from the figure, the single fixed point is stable for $a_6 \in (0, 1.1040)$. As the parameter a_6 increases from 0, the map undergoes a Neimark-Sacker bifurcation at $a_6 = 1.1040$, and the stable fixed point bifurcates into a quasi-periodic attractor. As the parameter a_6 decreases from 1.1040, the map undergoes a period-doubling bifurcation at $a_6 = 0$, and the stable fixed point bifurcates into a period-2 orbit. Thus, at $a_6 = 0$, the fixed point is non-hyperbolic. It should be noted that there are two coexisting attractors, a short regime of chaotic and quasi-periodic attractors. As the parameter a_6 decreases further, the stability of this fixed point changes. The Lyapunov exponents of the map SNFII_3 shown in Fig. 5(b) can demonstrate this numerical results.

From the bifurcation analyses of the maps SNFII_1 and SNFII_3 , we can conclude that the single fixed point is non-hyperbolic when the map undergoes a Neimark-Sacker or a period-doubling bifurcation, and meanwhile, the map has chaotic attractors.

4 Conclusions

Some elementary quadratic chaotic maps with a single non-hyperbolic fixed point were explored in this paper by performing an exhaustive computer search. Several typical examples of the two-dimensional maps were studied, and their typical attractors were shown in the phase-basin portraits and numerically analyzed by using the Lyapunov exponents and the the maximum of the local Lyapunov (Kaplan-Yorke) dimension. Our investigation indicates that there is no repelling

fixed point, so the Marotto's theorem is invalid. In order to investigate the occurrence of the chaotic attractor with a single non-hyperbolic fixed point, bifurcation analyses with respect to the parameter a_6 were carried out. The future works of this research will be to explore the chaotic attractors with a single non-hyperbolic fixed point in high-dimensional maps, and to propose the method for proving the existence of chaos in the maps with a single non-hyperbolic fixed point.

Acknowledgements

The authors are grateful to the anonymous reviewers for their valuable comments and suggestions that have helped to improve the presentation of the paper. This work is partially supported by the National Natural Science Foundation of China (Grant nos. 11402224 and 11672257), the Natural Science Foundation of Jiangsu Province of China (Grant nos. BK20161314 and BK20151295). We also thank Dr. Yang Liu and Dr. Zhouchao Wei for helpful comments.

References

- [1] G.A. Leonov and N.V. Kuznetsov. Hidden attractors in dynamical systems: From hidden oscillation in Hilbert-Kolmogorov, Aizerman and Kalman problems to hidden chaotic attractor in Chua circuits. *Int. J. Bifurc. Chaos*, 23 (2013): 1330002.
- [2] G.A. Leonov, N.V. Kuznetsov and V.I. Vagaitsev. Localization of hidden Chua's attractors. *Phys. Lett. A*, 375 (2011): 2230–2233.
- [3] G.A. Leonov, N.V. Kuznetsov and V.I. Vagaitsev. Hidden attractor in smooth Chua system. *Physica D*, 241 (2012): 1482–1486.
- [4] G.A. Leonov, N.V. Kuznetsov, M.A. Kiseleva, E.P. Solovyeva and A.M. Zaretskiy. Hidden oscillations in mathematical model of drilling system actuated by induction motor with a wound rotor. *Nonlinear Dyn.*, 77 (2014): 277–288.
- [5] G.A. Leonov, N.V. Kuznetsov, O.A. Kuznetsova, S.M. Seldedzhi and V.I. Vagaitsev. Hidden oscillations in dynamical systems. *Trans. Syst. Contr.*, 6 (2011): 54–67.
- [6] E.N. Lorenz. Deterministic Nonperiodic Flow. *J. Atmos. Sci.*, 20 (1963): 130–141.
- [7] O.E. Rossler. An equation for hyperchaos. *Phys. Lett. A*, 71 (1979): 155–157.
- [8] J.C. Sprott. Some simple chaotic flows. *Phys. Rev. E*, 50 (1994): 647–650.
- [9] L.O. Chua, M. Komuro and T. Matsumoto. The double scroll family. *IEEE Trans. Circuits Syst.*, 33 (1986): 1073–1118.
- [10] Z. Wang, S. Cang, E.O. Ochola EO and Y. Sun. A hyperchaotic system without equilibrium. *Nonlinear Dyn.*, 69 (2012): 531–537.
- [11] Z. Wei. Dynamical behaviors of a chaotic system with no equilibria. *Phys. Lett. A*, 376 (2011): 102–108.
- [12] Z. Wei, R. Wang and A. Liu. A new finding of the existence of hidden hyperchaotic attractor with no equilibria. *Math. Comput. Simul.*, 100 (2014): 13–23.
- [13] S. Jafari, J.C. Sprott and S.R.R.H. Golpayegani. Elementary quadratic chaotic flows with no equilibria. *Phys. Lett. A* 377 (2013): 699–702.
- [14] Z. Wei and Q. Yang. Dynamical analysis of a new autonomous 3-D system only with stable equilibria. *Nonlinear Anal. Real World Appl.*, 12 (2011): 106–118.
- [15] X. Wang and G. Chen. A chaotic system with only one stable equilibrium. *Commun. Nonlinear Sci. Numer. Simulat.* 17 (2012): 1264–1272.
- [16] M. Molate, S. Jafari, J.C. Sprott and S. Golpayegani. Simple chaotic flows with one stable equilibrium. *Int. J. Bifurc. Chaos*, 23 (2013): 1350188.
- [17] Z. Wei and W. Zhang. Hidden hyperchaotic attractors in a modified Lorenz-Stenflo system with only one stable equilibrium. *Int. J. Bifurc. Chaos*, 24 (2014): 1450127.
- [18] S. Jafari and J.C. Sprott. Simple chaotic flows with a line equilibrium. *Chaos Solitons Fractals*, 57 (2013): 79–84.
- [19] X. Wang and G. Chen. Constructing a chaotic system with any number of equilibria. *Nonlinear Dyn.*, 71 (2013): 429–436.
- [20] Y. Chen and Q. Yang. A new Lorenz-type hyperchaotic system with a curve of equilibria. *Math. Comput. Simul.*, 112 (2015): 40–55.

- [21] D. Dudkowski, S. Jafari, T. Kapitaniak, N.V. Kuznetsov, G.A. Leonov and A. Prasad. Hidden attractors in dynamical systems. *Phys. Rep.*, 637 (2016): 1–50.
- [22] F. Yu, P. Li, K. Gu and B. Yin. Research progress of multi-scroll chaotic oscillators based on current-mode devices. *Optik*, 127 (2016): 5486–5490.
- [23] V.-T. Pham, S. Vaidyanathan, C. Volos, S. Jafari and S.T. Kingni. A no-equilibrium hyperchaotic system with a cubic nonlinear term. *Optik*, 127 (2016): 3259–3265.
- [24] Z. Wang, J. Ma, S. Cang, Z. Wang and Z. Chen. Simplified hyper-chaotic systems generating multi-wing non-equilibrium attractors. *Optik*, 127 (2016): 2424–2431.
- [25] V.-T. Pham, C. Volos and T. Kapitaniak. *Systems with Hidden Attractors From Theory to Realization in Circuits*. Springer, Berlin. 2017.
- [26] W.P. Heatha, J. Carrasco and M. Senb. Second-order counterexamples to the discrete-time Kalman conjecture. *Automatica*, 60 (2015): 140–144.
- [27] S. Jafari, V.-T. Pham, M. Moghtadaei and S.T. Kingni. The relationship between chaotic maps. *Int. J. Bifurc. Chaos*, 26 (2016): 1650211.
- [28] H.B. Jiang, Y. Liu, Z. Wei and L.P. Zhang. Hidden chaotic attractors in a class of two-dimensional maps. *Nonlinear Dyn.*, 85 (2016): 2719–2727.
- [29] H.B. Jiang, Y. Liu, Z. Wei and L.P. Zhang. A new class of three-dimensional maps with hidden chaotic dynamics. *Int. J. Bifurc. Chaos*, 26 (2016): 1650206.
- [30] D. Dudkowski, A. Prasad and T. Kapitaniak. Perpetual points and periodic perpetual loci in maps. *Chaos*, 26 (2016): 103103.
- [31] T. Kapitaniak and G.A. Leonov. Multistability: unconvincing hidden attractors. *Eur. Phys. J. Special Topics*, 224 (2015): 1405–1408.
- [32] L.P. Shilnikov. A case of the existence of a countable number of periodic motions. *Sov. Math. Doklady*, 6 (1965): 163–166.
- [33] L.P. Shilnikov, A.L. Shilnikov, D.V. Turaev and L.O. Chua. *Methods of Qualitative Theory in Nonlinear Dynamics*. World Scientific, Singapore. 1998.
- [34] Z. Wei, J.C. Sprott and H. Chen. Elementary quadratic chaotic flows with a single non-hyperbolic equilibrium. *Phys. Lett. A*, 379 (2015): 2184–2187.
- [35] T.Y. Li and J.A. Yorke. Period three implies chaos. *Amer. Math. Monthly*, 82 (1975): 985–992.
- [36] F.R. Marotto. Snap-back repellers imply chaos in R^n . *J. Math. Anal. Appl.*, 63 (1978) 199–223.
- [37] C.P. Li and G. Chen. An improved version of the Marotto theorem. *Chaos Solitons Fractals*, 18 (2003): 69–77.
- [38] C.P. Li and G. Chen. On the Marotto-Li-Chen theorem and its application to chaotification of multi-dimensional discrete dynamical systems. *Chaos Solitons Fractals*, 18 (2003): 807–817.
- [39] F.R. Marotto. On redefining a snap-back repeller. *Chaos Solitons Fractals*, 25 (2005): 25–28.
- [40] C.C. Peng. Numerical computation of orbits and rigorous verification of existence of snapback repellers. *Chaos*, 17 (2007): 013107.
- [41] M.C. Li and M.J. Lyu. A simple proof for persistence of snap-back repellers. *J. Math. Anal. Appl.*, 352 (2009): 669–671.
- [42] K.L. Liao and C.W. Shih. Snapback repellers and homoclinic orbits for multi-dimensional maps. *J. Math. Anal. Appl.*, 386 (2012): 387–400.
- [43] Z. Elhadj and J.C. Sprott. Some criteria for chaos and no chaos in the quadratic map of the plane. *Ser. Elec. Energ.*, 22 (2009): 105–117.
- [44] Q.D. Li and X.S. Yang. A simple method for finding topological horseshoes. *Int. J. Bifurc. Chaos*, 20 (2010): 467–478.
- [45] Z. Galias and W. Tucker. Is the Henon attractor chaotic?. *Chaos*, 25 (2015): 033102.
- [46] J.C. Sprott. *Elegant Chaos: Algebraically Simple Chaotic Flows*. World Scientific, Singapore. 2010.
- [47] J.C. Sprott. *Strange Attractors: Creating Patterns in Chaos*. M&T books, New York. 2000.
- [48] Y.A. Kuznetsov. *Elements of Applied Bifurcation Theory (2ed)*. Springer-Verlag, New York. 1998.
- [49] Z. Elhadj and J.C. Sprott. *2-D Quadratic Maps and 3-D ODE Systems: a Rigorous Approach*. World Scientific, Singapore. 2010.
- [50] A.C.J. Luo. *Discrete and Switching Dynamical Systems*. Higher Education Press, Beijing. 2012.
- [51] A. Medio and M. Lines. *Nonlinear Dynamics a Primer*. Cambridge University Press, Cambridge. 2002.
- [52] P. Frederickson, J.L. Kaplan, E.D. Yorke and J.A. Yorke. The Lyapunov dimension of strange attractors. *J. Differ-*

ential Equations, 49 (1983): 185–207.

- [53] N.V. Kuznetsov and G.A. Leonov. A short survey on Lyapunov dimension for finite dimensional dynamical systems in Euclidean space. <http://arxiv.org/pdf/1510.03835v2.pdf> (2015).
- [54] G.A. Leonov, N.V. Kuznetsov and T.N. Mokaev. Homoclinic orbits, and self-excited and hidden attractors in a Lorenz-like system describing convective fluid motion. *Eur. Phys. J. Special Topics*, 224 (2015): 1421–1458.
- [55] N.V. Kuznetsov, T.N. Mokaev and P.A. Vasilev. Numerical justification of Leonov conjecture on Lyapunov dimension of Rossler attractor. *Commun. Nonlinear Sci. Numer. Simulat.*, 19 (2014): 1027–1034.
- [56] N.V. Kuznetsov, T.A. Alexeeva and G.A. Leonov. Invariance of Lyapunov exponents and Lyapunov dimension for regular and irregular linearizations. *Nonlinear Dyn.*, 85 (2016): 195–201.
- [57] N.V. Kuznetsov. The Lyapunov dimension and its estimation via the Leonov method. *Phys. Lett. A*, 380 (2016): 2142–2149.